Full-order anti-windup design with pole-placement constraints

Matthew C. Turner
Dept. of Engineering
University of Leicester

21/04/2017

1 Introduction

A control system which is linear apart from saturation of the control signal, and equipped with an anti-windup compensator, experiences three modes of operation:

- **Mode I** - Linear behaviour. If the control signal lies below the saturation threshold, no nonlinear behaviour will occur and the system will behave as a linear system, with behaviour determined by the nominal controller
- **Mode II** - Saturated behaviour. The control signal will be above the saturation threshold and the anti-windup compensator will be active. This regime is nonlinear and the system's behaviour is determined by the plant, controller and anti-windup compensator dynamics. The anti-windup compensator can be considered to be in closed-loop.
- **Mode III** - Recovery from saturation. The control signal has fallen below the saturation threshold, with the anti-windup compensator influencing the behaviour of the system by its exponentially decaying inputs into the controller.

During Mode III behaviour, when the system is recovering from a saturation event, the anti-windup compensator functions in an open-loop manner. This is unlike during Mode II, when saturation is active, and the anti-windup compensator behaves in a closed-loop manner. To ensure recovery of linear behaviour during Mode III, it is desirable to have some control over the anti-windup compensator's poles so that a graceful return of linear behaviour can be achieved.

It is interesting to note that many anti-windup techniques have concentrated on optimisation of Mode II behaviour, that is the *closed-loop* behaviour of the system *during* saturation. Unfortunately an anti-windup compensator which achieves optimal Mode II behaviour may contain poles which could be too fast, too slow or too poorly damped: either case could be problematic for Mode III behaviour or, in the case of fast poles, for implementation. While some indirect control of the anti-windup compensator's poles may be achieved by adjusting the various weighting matrices - and this is particularly true of the Riccati approach [4] - direct influence over the compensator's pole cannot be exerted using the standard full-order approaches.
Therefore, the aim of this note is to describe how a full-order LMI-based mismatch compensator can be designed subject to constraints on its pole locations. The technique is quite simple and consists of augmenting existing full-order anti-windup routines with pole-placement constraints taken from the LMI literature (see [2]). This leads to a convex design procedure for the anti-windup compensator. It is important to note the following key limitations inherent with this approach

- With a given set of pole-placement constraints, the full-order anti-windup design problem may not be feasible. This is because the standard full-order design algorithm may require the poles to be placed in a certain region in order to ensure nonlinear stability (effectively to meet the Circle Criterion). If the region specified by the pole placement constraints does not include this, the problem will be infeasible.

- Even if the anti-windup design problem is feasible, the compensator produced by the method described here is likely to be sub-optimal in terms of $\mathcal{L}_2$ performance during Mode II. The full-order compensator (it can be proven) will deliver optimal $\mathcal{L}_2$ performance when its poles are unconstrained. When its poles are constrained, this performance may deteriorate, although how much can only be assessed on a case-by-case basis. A similar observation was made about low-order compensators [6].

- The approach given here is more flexible than the low-order approaches of [6, 1] because the poles are *not fixed*, but are simply constrained to lie in a given region. This should give a better trade-off between Mode II and Mode III performance, but obviously it will typically result in a compensator with a higher-order than might be obtainable with the algorithms in [6, 1]. Note also that the approach to be described here is also more straightforward and should require less iteration than the low-order approaches.

2 LMI regions

The regions considered for pole locations are regions in the complex plane described by the following equation

$$\mathcal{D} = \{z \in \mathbb{C} : \quad f_D(z) < 0\} \tag{1}$$

where

$$\begin{aligned} f_D(z) &= \alpha + z\beta + \beta' z^* & (2)\\ &= [\alpha_{kl} + \beta_{kl} z + \beta lkz^*]_{1\le k,l\le m} & (3) \end{aligned}$$

where $\alpha = \alpha' \in \mathbb{R}^{m\times m}$ is a symmetric matrix and $\beta \in \mathbb{R}^{m\times m}$. The main result of [2] states that the poles of a matrix $A \in \mathbb{R}^{n\times n}$ are located in the region $\mathcal{D}$ if there exists a positive definite symmetric matrix $X > 0$ such that

$$M_{\mathcal{D}}(A, X) < 0 \tag{4}$$

where

$$\begin{aligned} M_{\mathcal{D}}(A, X) &= \alpha \otimes X + \beta \otimes (AX) + \beta' \otimes (AX)' & (5)\\ &= [\alpha_{kl} X + \beta_{kl} AX + \beta_{lk} XA']_{1\le k,l\le m} & (6) \end{aligned}$$

2.1 Sample LMI regions

2.1.1 Real part of poles less than $-\epsilon$

In this case, the region $\mathcal{D}$ is described by

$$\mathcal{D} = \{z \in \mathbb{C} : \quad \Re(z) < -\epsilon\} \tag{7}$$

To convert this into an LMI region, note that for a complex number $z = x + jy$, we have

$$\Re(z) = x = \frac{z}{2} + \frac{z^*}{2} \tag{8}$$

So $\Re(z) < -\epsilon$ is equivalent to

$$\begin{aligned} \frac{z}{2} + \frac{z^*}{2} &< -\epsilon & (9)\\ \Leftrightarrow z + z^* &< -2\epsilon & (10)\\ 2\epsilon + z + z^* &< 0 & (11) \end{aligned}$$

which now has the form of f_D with $\alpha = 2\epsilon I$ and $\beta = \beta' = 1$.

2.1.2 Disc of radius r centered at origin

In this case, the region $\mathcal{D}$ is described by

$$\mathcal{D} = \{z \in \mathbb{C} : \quad |z| < r\} \tag{12}$$

Note that

$$\begin{aligned} |z| < r &\Leftrightarrow z^*z < r^2 && (13)\\ &\Leftrightarrow z^*z - r^2 < 0 && (14)\\ &\Leftrightarrow \frac{z^*z}{r} - r < 0 && (15)\\ & && (16) \end{aligned}$$

Using the Schur complement, this is equivalent to

$$\begin{bmatrix} -r & z \\ z^* & -r \end{bmatrix} < 0 \tag{17}$$

which can be expressed as

$$\begin{bmatrix} -r & 0 \\ 0 & -r \end{bmatrix} + \begin{bmatrix} 0 & 1 \\ 0 & 0 \end{bmatrix} z + \begin{bmatrix} 0 & 0 \\ 1 & 0 \end{bmatrix} z^* \tag{18}$$

which again has the form of f_D as required.

2.1.3 Sector of left-half complex plane centered at the origin

In this case, the region $\mathcal{D}$ is described by

$$\mathcal{D} = \{z \in \mathbb{C} : (\tan\theta)x < -|y|\} \tag{19}$$

First note again that

$$x = \frac{z}{2} + \frac{z^*}{2}$$

Next note that

$$(z - z^*)(z - z^*) = (2jy)(2jy) = -4|y|^2 \tag{20}$$

So

$$\begin{aligned} |y|^2 &= \frac{(z - z^*)(z - z^*)}{-4} && (21)\\ |y| &= \frac{\sqrt{-(z - z^*)(z - z^*)}}{2} && (22)\\ -|y| &= -\frac{\sqrt{-(z - z^*)(z - z^*)}}{2} && (23) \end{aligned}$$

Therefore $(\tan\theta)x < -|y|$ is equivalent to

$$\tan\theta\left(\frac{z}{2}+\frac{z^*}{2}\right) < -\frac{\sqrt{-(z-z^*)(z-z^*)}}{2} \tag{24}$$

$$\Leftrightarrow \quad \tan\theta(z+z^*) < -\sqrt{-(z-z^*)(z-z^*)} \tag{25}$$

$$\Leftrightarrow \quad \tan^2\theta(z+z^*)(z+z^*) < -(z-z^*)(z-z^*) \tag{26}$$

$$\Leftrightarrow \quad \sin^2\theta(z+z^*)(z+z^*) < \cos^2\theta(z^*-z)(z-z^*) \tag{27}$$

$$\Leftrightarrow \quad \sin\theta(z+z^*) < \frac{\cos^2\theta(z^*-z)(z-z^*)}{\sin\theta(z+z^*)} \tag{28}$$

$$\Leftrightarrow \quad \sin\theta(z+z^*) - \frac{\cos^2\theta(z^*-z)(z-z^*)}{\sin\theta(z+z^*)} < 0 \tag{29}$$

Using the Schur complement this becomes

$$\begin{bmatrix} \sin\theta(z+z^*)(\theta) & \cos(\theta)(z^*-z) \\ \cos(\theta)(z^*-z)^* & \sin\theta(z+z^*) \end{bmatrix} < 0 \tag{30}$$

which can be written as

$$\begin{bmatrix} \sin\theta & -\cos(\theta) \\ \cos(\theta) & \sin\theta \end{bmatrix} z + \begin{bmatrix} \sin\theta & \cos(\theta) \\ -\cos(\theta) & \sin\theta \end{bmatrix} z^* < 0 \tag{31}$$

which has the form of $f_D(z)$

3 Application to anti-windup design

A full-order coprime factor-based anti-windup compensator [5] has the following state-space description

$$\left[\begin{array}{c} \dot{x} \\ \hline u_d \\ y_d \end{array}\right] = \left[\begin{array}{c|c} A+BF & B \\ \hline F & 0 \\ C+DF & D \end{array}\right] \left[\begin{array}{c} x \\ \hline \mathrm{Dz}(u) \end{array}\right] \tag{32}$$

where the plant state-space realisation is $G(s) \sim (A, B, C, D)$ and F is the stabilising state-feedback matrix which determines the anti-windup compensator. Refer to [5] for full details. During Mode III behaviour, the control signal u has fallen below its limits so that $\mathrm{Dz}(u) = 0$ and the system can be considered as evolving in time from a state reached at time t_1 which is assumed to be when Mode III behaviour has begun. The dynamics are thus described by

$$\dot{x} = (A+BF)x \quad x(t_1) = x_0 \tag{33}$$

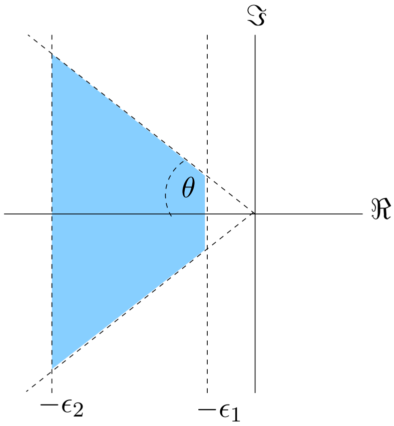

Figure 1: Pole location in complex plane. The region of interest, the intersection of $\mathcal{D}_i$ is highlighted in blue.

It follows that, during Mode III behaviour, we are therefore interested in placing the poles of the matrix $(A + BF)$ in a desired region so that the state of the compensator converges in a sufficiently graceful manner.
It is probably sufficient to place the poles in a region of the complex plane where the real part of the poles is not too large or too small and the damping of the poles is not too low. This region can be described by the intersection of a sector centered at the origin and two half-planes, one such that $\Re(z) < -\epsilon_1$ and the other such that $\Re(z) > -\epsilon_2$. This region is shown in Figure 1. This requires the poles to be located at the intersection of the following LMI regions:

$$\mathcal{D}_1 = \{z \in \mathbb{C} : \quad \Re(z) < -\epsilon_1\} \tag{34}$$
$$\mathcal{D}_2 = \{z \in \mathbb{C} : \quad \Re(z) > -\epsilon_2\} \tag{35}$$
$$\mathcal{D}_3 = \{z \in \mathbb{C} : (\tan\theta)x < -|y|\} \tag{36}$$

where θ determines the minimum damping of the poles. The associate $f_{\mathcal{D}}$ functions are:

$$f_{\mathcal{D}_1} = 2\epsilon_1 + z + z^* < 0 \tag{37}$$
$$f_{\mathcal{D}_2} = -2\epsilon_2 - z - z^* < 0 \tag{38}$$
$$f_{\mathcal{D}_3} = \begin{bmatrix} \sin\theta & -\cos(\theta) \\ \cos(\theta) & \sin\theta \end{bmatrix} z + \begin{bmatrix} \sin\theta & \cos(\theta) \\ -\cos(\theta) & \sin\theta \end{bmatrix} z^* < 0 \tag{39}$$
$$\tag{40}$$

This then yields the following LMI's

$$M_{\mathcal{D}_1}(A+BF,X_1) = 2\epsilon_1 X_1 + (A+BF)X_1 + X_1(A+BF)' < 0 \tag{41}$$

$$M_{\mathcal{D}_2}(A+BF,X_2) = -2\epsilon_2 X_2 - (A+BF)X_2 - X_2(A+BF)' < 0 \tag{42}$$

$$M_{\mathcal{D}_3}(A+BF,X_3) = \begin{bmatrix} \sin\theta(A+BF)X_3 & -\cos(\theta)(A+BF)X_3 \\ \cos(\theta)(A+BF)X_3 & \sin\theta(A+BF)X_3 \end{bmatrix} \begin{bmatrix} \sin\theta X_3(A+BF)' & \cos(\theta)X_3(A+BF)' \\ -\cos(\theta)X_3(A+BF)' & \sin\theta X_3(A+BF)' \end{bmatrix} < 0 \tag{43}$$

Note that $M_{\mathcal{D}_3}(A+BF,X_3)$ can be simplified to

$$M_{\mathcal{D}_3}(A+BF,X_3) = \begin{bmatrix} \sin\theta[(A+BF)X_3 + X_3(A+BF)'] & \cos(\theta)[(A+BF)X_3 - X_3(A+BF)'] \\ \cos(\theta)[X_3(A+BF)' - (A+BF)X_3] & \sin\theta[(A+BF)X_3 + X_3(A+BF)'] \end{bmatrix} \tag{44}$$

Irrespective of the other inequalities which need to be solved in order to guarantee closed-loop nonlinear stability and performance during Mode III, it can be seen that, with F as a design parameter, these inequalities are not jointly convex in the variables, X_1, X_2, X_3 and F. However, letting $Q = X_1 = X_2 = X_3$ and using the substitution $L = FQ$, one can transform the inequalities into

$$2\epsilon_1 Q + AQ + QA' + BL + L'B' < 0 \tag{45}$$

$$-2\epsilon_2 Q - AQ - QA' - BL - L'B' < 0 \tag{46}$$

$$\begin{bmatrix} \sin\theta[AQ + QA' + BL + L'B'] & \cos(\theta)[AQ - QA' + BL - L'B'] \\ \cos(\theta)[AQ - QA' + BL - L'B']' & \sin\theta[AQ + QA' + BL + L'B'] \end{bmatrix} < 0 \tag{47}$$

These inequalities are convex in Q and L and their satisfaction will ensure that the poles of $A + BF$ are located in the desired region. Note that this convexification comes at a price: conservatism. In fact the fewer constraints on closed-loop pole position, the lower the conservatism and also the higher likelihood of achieving better Mode II performance.

3.1 A pole-placement anti-windup design algorithm

Note that the inequalities listed above only enforce constraints on the anti-windup compensator's closed-loop poles; they do not guarantee nonlinear stability or performance. However, they can be appended to the design procedure in [5], where linear matrix inequalities are given which ensure (for

Algorithm 1 LMI-Based Design Algorithm with pole constraints

1. Choose weighting matrices $W_p > 0$ (performance) and $W_r > 0$ (robustness)

2. Choose $\epsilon_1 > 0, \epsilon_2 > 0$ and $\theta \in [0, \pi/2]$

3. Solve the following LMI-optimisation problem:

   $\min \gamma$ subject to

$$\begin{bmatrix} QA' + AQ + L'B' + BL + 2\epsilon_1 Q & BU - L' & 0 & QC' + L'D' & L' \\ \star & -2U & I & UD' & U \\ \star & \star & -\gamma I & 0 & -I \\ \star & \star & \star & -\gamma W_p^{-1} & 0 \\ \star & \star & \star & \star & -\gamma W_r^{-1} \end{bmatrix} < 0 \tag{48}$$

$$-2\epsilon_2 Q - AQ - QA' - BL - L'B' < 0 \tag{49}$$

$$\begin{bmatrix} \sin\theta[AQ + QA' + BL + L'B'] & \cos(\theta)[AQ - QA' + BL - L'B'] \\ \cos(\theta)[AQ - QA' + BL - L'B']' & \sin\theta[AQ + QA' + BL + L'B'] \end{bmatrix} < 0 \tag{50}$$

   where $Q > 0$, $U > 0$ (and diagonal) and L are matrix variables

4. Construct $F = LQ^{-1}$

5. Form the anti-windup compensator using the state-space realisation (32).

---

stable plants at least) the overall nonlinear system is stable and the deviation between linear and saturated behaviour satisfies an $\mathcal{L}_2$ gain condition. Therefore, an anti-windup compensator ensuring nonlinear stability and performance and also satisfying the pole-placement constraints described above can be designed according to Algorithm 1.

In this algorithm, the constraint on the maximum value of the real part of the poles of $(A + BF)$ has been incorporated into the LMI ensuring nonlinear stability and $\mathcal{L}_2$ gain; thus LMI (45) does not appear in isolation in Algorithm 1. It is again noted that this algorithm is conservative because it uses the same "Lyapunov" matrix to enforce pole constraints and nonlinear stability and performance. In fact, for arbitrary choices of ϵ_1, ϵ_2 and θ the LMI's in Algorithm 1 may not be feasible. It is therefore advisable to introduce them iteratively and to gradually tighten the pole constraints; in addition, if one constraint is tightened, feasibility may only be recovered if another is relaxed e.g. tight constraints in damping (a small value of θ) might only be achieved for very loose constraints on the location of the real part of the compensators poles, determined by ϵ_1 and ϵ_2.

3.2 Local anti-windup

In the case that the plant is not asymptotically stable, no *globally stabilising* anti-windup compensator exists so one must be content to ensure local asymptotic stability. This is incorporated into the design algorithms in a fairly straightforward manner here by using the *sector narrowing approach.* In this case (see example [5]), it is assumed that, locally, the deadzone is sector bounded within a narrower sector:

$$\mathrm{Dz} \in \mathrm{Sector}[0, \epsilon I] \quad \epsilon \in (0, 1]$$

When $\epsilon = 1$, global results are recovered; anything less than unity corresponds to local results. In this case, one can derive a similar synthesis algorithm for anti-windup design ensuring local asymptotic stability. This is stated in Algorithm 2 below; the crucial difference is that the designer must choose another scalar, $\epsilon \in (0, 1]$ which then is used in the main LMI in the algorithm. In fact, if the system has multiple control inputs, ϵ can be replaced by a diagonal matrix $\mathcal{A}$ in which all the elements are in the interval $(0, 1]$, reflecting possible differences in the sector which each individual deadzone occupies (locally). Note that if the plant is not asymptotically stable (which will be the case for rate-limit design), ϵ must be chosen strictly less than one.

Algorithm 2 LMI-Based Design Algorithm with pole constraints

1. Choose weighting matrices $W_p > 0$ (performance) and $W_r > 0$ (robustness)

2. Choose $\epsilon \in (0, 1]$

3. Choose $\epsilon_1 > 0, \epsilon_2 > 0$ and $\theta \in [0, \pi/2]$

4. Solve the following LMI-optimisation problem:

   $\min \gamma$ subject to

$$\begin{bmatrix} QA' + AQ + L'B' + BL + 2\epsilon_1 Q & BU - \epsilon L' & 0 & QC' + L'D' & L' \\ \star & -2U & \epsilon I & UD' & U \\ \star & \star & -\gamma I & 0 & -I \\ \star & \star & \star & -\gamma W_p^{-1} & 0 \\ \star & \star & \star & \star & -\gamma W_r^{-1} \end{bmatrix} < 0 \tag{51}$$

$$-2\epsilon_2 Q - AQ - QA' - BL - L'B' < 0 \tag{52}$$

$$\begin{bmatrix} \sin\theta[AQ + QA' + BL + L'B'] & \cos(\theta)[AQ - QA' + BL - L'B'] \\ \cos(\theta)[AQ - QA' + BL - L'B']' & \sin\theta[AQ + QA' + BL + L'B'] \end{bmatrix} < 0 \tag{53}$$

   where $Q > 0$, $U > 0$ (and diagonal) and L are matrix variables

5. Construct $F = LQ^{-1}$

6. Form the anti-windup compensator using the state-space realisation (32).

3.3 Illustrative example

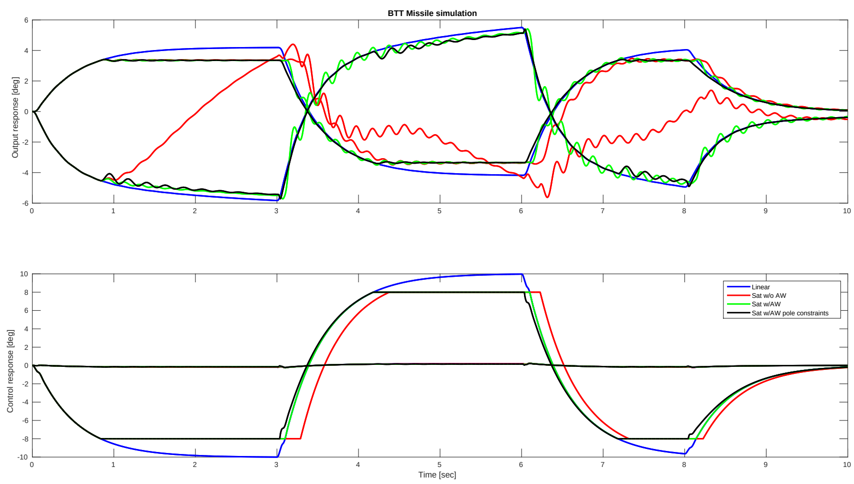

Figure 2: Simulation example. Control inputs are limited to $\pm$ 8 units.

To illustrated the use of pole constraints in anti-windup compensation we use the "missile"[1] example of [3] (see also [6]. A standard full-order anti-windup compensator was designed according to the technique of [5] using $W_p = I_2$ and $W_r = 100 \times I_2$. This compensator was 3rd order (since the plant was 3rd order) and the compensator had the following closed-loop poles:

$$\mathbf{spec}(A + BF) = \{-1.3981 + 32.2737j, -1.3981 - 32.2737j, -57.5118\}$$

Note that two of these poles are very lightly damped.
Another anti-windup compensator was designed, using Algorithm 1 with $\epsilon_1 = 0.001$, $\epsilon_2 = 2000$ and $\theta = 0.6\pi/2$. This produced a compensator with a similar $\mathcal{L}_2$ gain to the first compensator (with unconstrained) poles, but in this case the compensator's spectrum was

$$\mathbf{spec}(A + BF) = \{-1908.9, -4.8, -117.9\}$$

While these poles are faster than before, they are all real and thus one would expect, during Mode III, that the compensator would allow a more graceful return to linear behaviour.
Figure 2 shows some sample simulation results for the example, in which a series of pulses was used as a reference signal. The top sub-figure shows the

[1] It is not claimed here that this represents a realistic missile example, but it is useful to illustrate the ideas

two plant output and the bottom sub-figure shows the two control inputs. The linear response in blue is considered ideal. When the input is limited to ± 8 units in both channels, the control signal saturates and behaviour deteriorates; decoupling is compromised; this behaviour is shown in red. When standard full-order anti-windup, with no pole-placement constraints, is applied, the system behaves as indicated by the green traces: performance is much improved, but there is noticeable oscillation when saturation has ceased and Mode III begins. With the pole-placement anti-windup compensator (black), performance is similar during Mode II (or perhaps slightly worse), but the oscillation in Mode III is absent. In this case, some modest improvements have been made by using pole-placement constraints.

References

[1] J-M. Biannic, C. Roos, and S. Tarbouriech. A practical method for fixed-order anti-windup design. In 7^{th} *IFAC Symposium on Nonlinear Control Systems (NOLCOS)*, Pretoria, South Africa, 2007.

[2] M. Chilali and P. Gahinet. $\mathcal{H}_\infty$ design with pole placement constraints: an LMI approach. *IEEE Transactions on automatic control*, 41(3):358–367, 1996.

[3] A.A. Rodriguez and J. R. Cloutier. Control of a bank-to-turn missile with saturating actuators. *Proc. American Control Conference*, 1994.

[4] J. Sofrony, M.C. Turner, and I. Postlethwaite. Anti-windup synthesis using Riccati equations. *Int J Control*, 80(1):112–128, 2007.

[5] M.C. Turner, G. Herrmann, and I. Postlethwaite. Incorporating robustness requirements into anti-windup design. *IEEE T Automat Contr*, 52(10), 2007.

[6] M.C. Turner and I. Postlethwaite. A new perspective on static and low order anti-windup synthesis. *Int J Control*, 77(1):27–44, 2004.